JOURNAL OF MATERIALS SCIENCE: MATERIALS IN MEDICINE 1 (1990) 146–153

# The application of holography to examine plated fracture fixation systems

J. C. SHELTON, D. GORMAN*‡ and W. BONFIELD
*Department of Materials, Queen Mary and Westfield College, Mile End Road, London E1 4NS, UK and *Department of Mechanical and Offshore Engineering, Robert Gordons Institute of Technology, School Hill, Aberdeen, UK*

The determination of the real strain patterns across a plated fractured bone is important in developing alternative and improved fracture fixation devices. Bone is strain sensitive, and therefore controlling the displacement or strain at the fracture site or near the fracture plate will effect the bone's response to the fixator. Holographic interferometry is shown to be a useful technique for examining very small displacements, in particular relative displacements between two separate parts of the bone–screw–plate system. Relative movement between the bone ends can be reduced by angling an osteotomy, by interlocking a natural fracture or, most efficiently, by applying compression across the fractured bone ends. Increasing the number of fixation points from four to six reduces the slip between the plate and the bone.

## 1. Introduction

At present the system of rigid internal fracture fixation is the most efficient and reliable system for the fixation of fractures and is widely used. This situation is partially due to the intensive training given to the surgeons in how to approach fracture fixation using the equipment and the excellent support services provided by the manufacturers. However, it is not certain that rigid internal fixation produces the best conditions for fracture healing [1, 2]. The application of successful research to produce improved fracture fixation systems depends not only on altering the conditions at the fracture site, but also on developing new techniques for analysis of the fracture fixation system both *in vitro* and *in vivo*.

New designs of internal fracture fixation plates have been reported which have investigated the effects of changing the axial, torsional or bending stiffness, by varying either the geometry of the plates or their material properties [1, 3–5]. The changes have been assessed using animal models [6, 7], computer simulation and finite-element analysis [8–10] and by testing some of the systems in human clinical trials [11]. Although considerable data have been accumulated from these various tests, improvements of plate-and-screw fracture fixation devices require an improved knowledge of the properties of the plate–screw–bone structure.

Fracture fixation by internal plating does not use a plate in isolation, but employs a plate attached to a bone by between six and 14 screws, depending on the nature of the fracture. The properties of the total bone–screw–plate structure are of paramount importance in the clinical application. It is therefore important to consider the whole system as well as its constituent parts, and to be able to identify how a structure comprising screws, plate and the bone deforms.

Holographic interferometry is a possible way of investigating this particular problem. It allows a full-field view of the movement of an object when it is loaded. Double-exposure holographic interferometry is a static technique where the effect of applying a small load to the object can be seen by fringes that indicate an out-of-plane movement. A brief summary of holographic interferometry is included in Appendix A. Determining real stress and strain distributions in orthopaedic systems presents many problems. Force transducers have been used to measure the forces that act on a system, and strain gauges have been extensively used to measure the strain on discrete parts of the bone. However, the determination of the real strain distribution is difficult both experimentally and theoretically. Photoelasticity has been used, but this is possible only with homogeneous bone models. Holographic interferometry has been shown to be useful in determining the real strain distributions in an experimental situation. Investigations by holography produce a high-resolution image of the actual body without any contact at all; the deformations that are recorded are purely as a result of the loads that are applied to the object and are not, therefore, affected by the recording method. The accuracy of measurement available from the technique is useful when viewing fracture fixation systems, since only small displacements are necessary across the fracture site to influence the type of fracture healing that will occur. The sensitivity of the method depends on the

‡Present address: Department of Mechanical Engineering, Queen Mary and Westfield College, Mile End Road, London E1 4NS, UK.


0957–4530/90 $03.00 + .12 

geometrical arrangement that is used [12] and the wavelength of the laser light used.

Holography has been used to investigate the surface deformations of a variety of orthopaedic systems such as the effect of titanium alloy stems compared with cobalt chromium stems for use in total hip replacements [13], the effect of hip prostheses on the deformation of femora [14], the severity of wear on implant materials and devices [15], the transfer of loads across the tibia and fibula and through the ankle joint [16], the investigation of the deformations of teeth [17] and the analysis of how vertebrae deform under different conditions [18].

Some researchers have used double-exposure holography to investigate internal fracture fixation plates, and the behaviour of the plates screwed on to bone [14, 18–20]. The basic viability of the technique was demonstrated [14] and the application of a thicker plate was shown to increase the stiffness of the system when loaded in four-point bending. The effects of applying compression were compared using two techniques [19]: photoelasticity and holography. The two techniques were complementary, although few holographic results were presented. The effect of plating tibiae with fracture plates was investigated [14, 18, 20] by loading in cantilever bending; the lateral and medial directions were found to be stiffer than the anterior and posterior directions, whether the bone was plated or not. However, if an osteotomy was carried out on the bone, followed by plating, the structure was found to be considerably weakened; this effect was increased by removing the two inner screws of the plate closest to the fracture. It was also noticed that under the same loading conditions the deformations of the plate and the bone did not coincide between the two inner screws, as the plate deformed more than the bone. This has been the only previous work to describe, qualitatively and quantitatively, the effects of internal fracture fixation plates on tibiae. However, most of the analysis was restricted to the bending stiffness of the system rather than any other loading modes. It is clearly very important also to look at the response of a fracture plated system to torsional loading; the greatest relative deformation between the fracture ends is likely to occur under twisting. By investigating different loading arrangements, and altering the number of screws, the type of plate and the fracture gap in this work, a better interpretation of the important parameters has been gained.

The fringe pattern produced on a double-exposure hologram depends on all the individual components of the displacement present, i.e. the deformation, rotation and rigid-body translations of the object. One of the simplest methods for interpretation of the fringes, relating the displacement or deformation of the object to the fringes, is the zero-fringe method [21]. This is described in Appendix B.

It can be seen from Appendix B that the out-of-plane displacements are a function of the number of fringes between two points. The higher the density of the fringes is, or the narrower the spacing between the fringes, the greater the surface deformation of the specimen. The fringes actually indicate the out-of-plane displacement in the direction that bisects the illumination and viewing directions, and this is a component of the absolute displacement of the object. Double-exposure holograms can be interpreted using photographs of the holograms, rather than the holograms themselves.

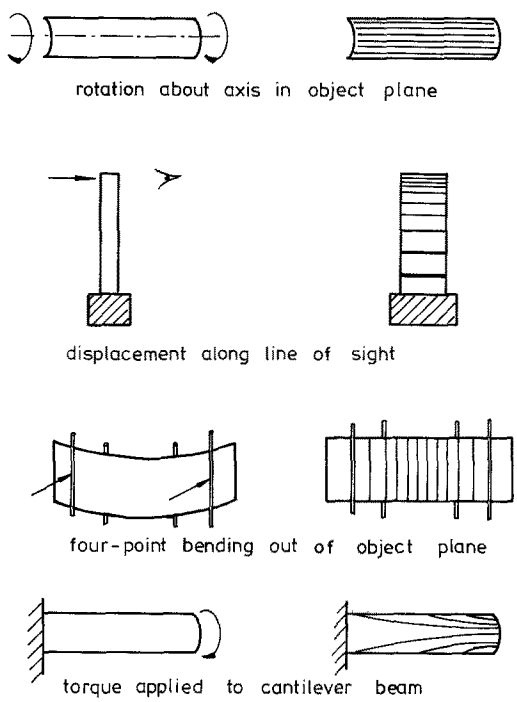


*Figure 1* Summary of typical fringe patterns for several loading conditions.

Fig. 1 shows a summary of the fringe patterns that are recorded under standard loading conditions. It may be used for a more qualitative approach to the problem. Qualitatively the technique is sensitive and its main application here has been in the comparison of the different fringe patterns that are produced under different loading conditions. The study presented here has developed the technique of double-exposure holographic interferometry to investigate the relative movement between the ends of a fractured bone or a bone with an osteotomy under loading, and to investigate the relative movement between other interfaces within the bone–screw–plate system. From these data it has been possible to investigate the relative stiffness of various fracture fixation configurations.

## 2. Experimental method

### 2.1. Experimental tests

Whole human tibiae obtained fresh from cadavers were cleaned on receipt, removing all tissue and periosteum from the shaft. The bones were stored at $-20°$ C. On retrieval from the freezer the bones were placed in Ringer's solution for at least 6 h, at room temperature, to ensure that the bone had completed defrosted and had fully rehydrated. The surface of the tibiae were dried and a thin layer of white water-resistant paint was sprayed over the entire mid-shaft surface. Bone is not a highly reflective material, and keeping it wet reduced the reflectivity. By coating the surface with this thin layer of paint the bone could be kept completely wet, while at the same time the

TABLE I Tibiae, fracture types and fixation method used in experimental tests

| Tibia | Plate thickness | Fastener | | Fracture | |
|---|---|---|---|---|---|
| | | Number | Diameter (mm) | Gap | Orientation (degrees) |
| 1 | 2 mm | 6 | 4.0 | 1 mm | 90 |
| 2 | 4 mm | 6 | 4.5 | 1 mm | 90 |
| 3 | 4 mm | 4 | 4.0 | 1 mm | 90 |
| 4 | 4 mm | 6 | 4.5 | Contact | 45 |
| 5 | 4 mm | 6 | 4.5 | Contact | Fractured |
| 6 | Osteo plate | 8 | 4.5 | Compression | 90 |
| 7 | AO plate | 10 | 4.5 | Compression | 90 |

surface could be wiped dry, reducing the amount of light that was scattered. In this way it became possible to record high-quality images on small pieces of photographic emulsion-coated glass.

A series of tibiae were tested as shown in Table I. The fracture fixation plates were made from orthopaedic grade stainless steel. The experimental plates were machined from barstock into rectangular plates 12 mm × 100 mm (or 70 mm) depending on whether the plate had four or six holes. The distance between the central screws was 30 mm and the rest 15 mm. The plates were either 2 or 4 mm thick as indicated in Table II. The holes in the plate were drilled to be clearance holes, for either 4 or 4.5 mm o.d. screws, depending on whether Sherman or AO screws were used. The AO and Osteo plates were both standard dynamic compression (3.8 mm thick) or autocompression plates (4 mm thick), respectively, with a curved cross-section.

## 2.2. Holographic test apparatus

The holographic apparatus, shown in Fig. 2, was located in a basement room on a cast iron vibration-isolated table, to improve structural and thermal stability and to allow the equipment to be clamped magnetically to it. The beam from the He–Ne continuous-wave gas laser (Spectra Physics Inc., USA, class IIIb, nominal power 10 mW, wavelength 632.8 nm) was split using a variable beamsplitter. The object beam was made divergent by passing it through a collimator. The wider beam was then reflected from the object and a diffuse wavefront was then incident on the photographic plate. The reference beam was reflected through two mirrors and then a collimator before falling on the photographic plate. Optical noise was removed by passing the beams through a pinhole. For the best results the ratio of the object to reference beam intensity was found to be 1 : 5 [22]. The amount of light reflected from the object varied depending on the specimen used and, therefore, a polarizing plate was placed along the reference beam to adjust its intensity to maintain this ratio. The light intensity of the two beams was measured using a light intensity meter. The plate holder was positioned so that the angle of incidence between the reference and object beam was the same and as close to perpendicular as possible. Both beams were adjusted to be the same length within the coherence of the laser. The glass plates coated with photographic emulsion (Agfa–Gevaert, Belgium, type 8E75AD) were high-sensitivity plates with a grainsize of approximately 35 nm, and a resolving power of 5000 lines $mm^{-1}$.

## 2.3. Recording procedure

Double-exposure holograms were taken in two ways. The bone was either loaded in three-point bending or in torsion. The load increments applied to the bone were varied according to the stiffness of the whole system. A fringe density was required that was visible while not being too coarse so that accuracy in interpreting the fringes was limited; this was found to be approximately 1 fringe $mm^{-1}$. At least three repeats of each double-exposure hologram were made. A manually operated shutter was used with each exposure made for between 3 and 4 sec. Before each exposure a delay of 5 sec allowed the system to become stable, while not permitting creep effects to become significant. The plates were then developed in Kodak D-19 developer and fixed before being returned to their original position. The reconstructed image with interference fringes could then be observed through the hologram illuminated by the reference beam only.

# 3. Results

Reconstructions of holograms of tibia 1 are shown in Fig. 3. The fringes run across the bone and the plates,

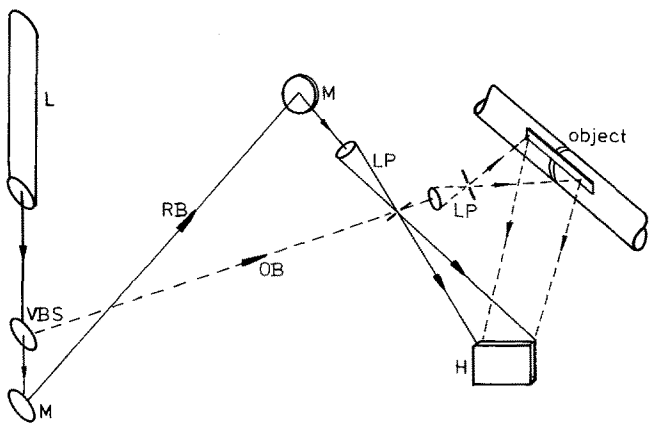


*Figure 2* Schematic of holographic set-up. L, Laser; VBS, variable beamsplitter; M, mirror; LP, lens pinhole combination; H, hologram; RB, reference beam; OB, object beam.

TABLE II Summary of fringe density ratio (FDR) values for tibiae

| Tibia | Gap | FDR ratio | Mean FDR ratio |
|---|---|---|---|
| 2 | 1 mm | 0.58 | |
| | | 0.48 | 0.50 |
| | | 0.46 | |
| 3 | 1 mm | 0.22 | |
| | | 0.22 | 0.22 |
| | | 0.21 | |
| 4 | Contact (45°) | 0.43 | |
| | | 0.43 | 0.43 |
| | | 0.44 | |
| 5 | Contact | 0.54 | |
| | | 0.36 | 0.54 |
| | | 0.43 | |
| 6 | Compression | 0.60 | |
| | | 0.70 | 0.62 |
| | | 0.56 | |
| 7 | Compression | 0.43 | |
| | | 0.44 | 0.45 |
| | | 0.49 | |

inclined at between 5 and 20° to the vertical relative to the edge of the fixation plate, indicating that the deformation that occurred was not true three-point bending (which would produce vertical lines). The fringes cross the plate–bone interface without disturbance away from the fracture site. Howver, closer to the fracture site fewer fringes are found on the plate than on the bone and the fringes are no longer continuous across the interface.

All of the subsequent double-exposure holography was carried out by incremental loading in torsion, applying a small torque to the right-hand side of the bone as viewed in the photographs, while the bone was rigidly built-in at the left-hand side. The torques that were applied varied according to the torsional stiffness of the system, from approximately 0.05 to 0.5 N m.

A hologram of tibia 2 is shown in Fig. 4. The fracture ends were set 1 mm apart, with the fracture repaired by a six-hole, 4 mm thick rectangular plate. The fringes are continuous on the right-hand (loaded) side of the tibia across the bone–plate interface. However, at the fracture site there is a sharp discontinuity in the fringe pattern. The fringe density becomes lower on the left-hand side and the fringes become angled relative to the edge of the plate. The angled fringes indicate that both twisting and bending were occurring on the plate and tibia, as shown in Fig. 1. The fringes are inclined at a steeper angle on the left-hand side of the bone than on the plate, indicating that the bone was experiencing less twisting than the plate.

A hologram of tibia 3 with a four-screw, 4 mm thick plate attached, is shown in Fig. 5. The fringes on the plate are not continuous with those on the bone; the

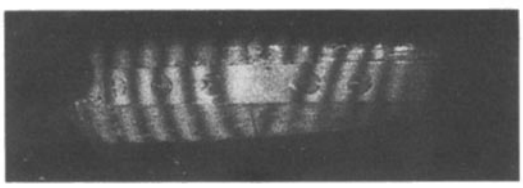

*Figure 3* Double-exposure hologram of tibia 1, under three-point loading. The discontinuity of fringes at the fracture site indicates relative movement between the plate and bone.

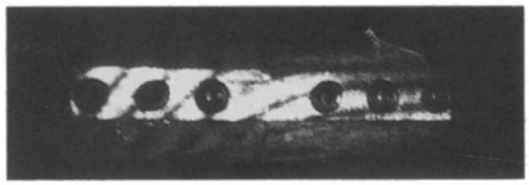

*Figure 4* Reconstructed image from hologram of tibia 2, under torsional loading, loaded as shown by arrows. The change in direction of fringes across the fracture site shows a change from a twisting mode to an out-of-plane bending.

difference in fringe density between the plate and the bone indicates that movement was occurring between the plate and the bone. The fringes are acutely angled relative to the edge of the plate as the load is transferred from the right- to the left-hand side, indicating that the plate is moving primarily in torsion rather than bending, and the loads transferred to the bone are also primarily torsional, although an increase in the angle of the fringes indicated that some bending was occurring.

Fig. 6 shows a result for tibia 4 with an osteotomy applied to the bone at an angle to the plane of viewing and fixed with a six-hole, 4 mm thick plate. The hologram shows that by inclining the fracture site, the transmission of bending to the right-hand side was almost entirely eliminated, although no compression had been applied.

An osteotomy is an extremely unnatural situation for a bone, as in natural fractures the bone ends are rough and may interlock if they are brought close to each other and hence increase the stability of the system. For this reason a fracture more indicative of an *in vivo* case was produced by loading tibia 5 in four-point bending to failure, producing a butterfly fragment on the tension side of the bone. Before attaching a plate the bone was reduced accurately and carefully in an attempt to interlock the fracture ends. Fig. 7 shows the front view of this natural fracture, and shows that even with no compression across the fracture site the bending effect on the right-hand side of the bone was eliminated.

Two clinically used compression plates were applied to two tibiae (6 and 7), as shown in Figs 8 and 9. Both plates were attached according to the manufacturers' instructions, with compression applied across the osteotomy by tightening the screws positioned eccentrically in the angulated holes, to bring the bone ends into contact. The fringes show much greater continuity across the fracture site than in any of the previous tests, indicating that much less relative movement was occurring between the fracture ends. Fig. 8 shows the eight-hole Osteo plate and the fringes on the right-

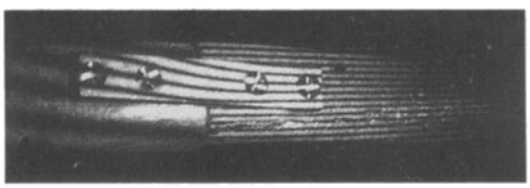

*Figure 5* Reconstructed image from hologram of tibia 3. There is a large change in fringe density at the fracture site as a result of fewer attachment points across plate to bone.

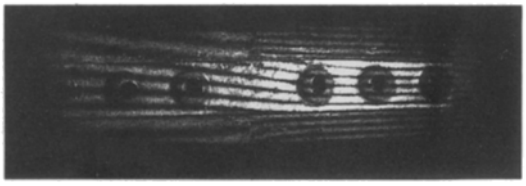

*Figure 6* Reconstructed image from hologram of tibia 4. Angled osteotomy reduces the out-of-plane movement, as shown by change in fringe direction.

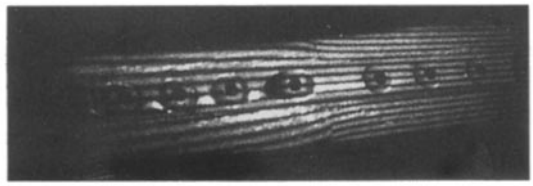

*Figure 8* Reconstructed image from hologram of tibia 6. Effective compression across the fracture site from Osteo plate reduced the relative movement of the fracture bone ends, as shown by the near continuity of fringes across fracture site.

hand side of the fracture run almost continuously across the fracture and then diverge slightly, as would be expected for an object loaded in pure torsion while built-in at the right-hand side. The fringes do not become angled relative to the plate, indicating that no bending has been applied to this tibia or plate. Fig. 9 shows an AO ten-holed, narrow, dynamic compression plate applied across an osteotomy. Again the fringes run fairly continuously across the fracture site, with little difference between the number of fringes on the right- and left-hand sides.

Some of the effects discussed so far can be quantified by introducing a ratio term for the relative fringe densities on either side of the fracture. This fringe density ratio (FDR) may be defined as

$$\text{FDR} = \frac{\text{mean separation of fringes on left-hand side of fracture}}{\text{mean separation of fringes on right-hand side of fracture}} \quad (1)$$

where the fringes are considered at the fracture site. This ratio provides an indication of the amount of torque that is transferred across the discontinuity, i.e. the effective stiffness of the bone–plate structure. According to the definition in Equation 1, the values of FDR for all the tibiae described earlier are shown in Table II. An FDR of unity indicates a perfect fracture repair, as the fringes show no difference in spacing either side of the fracture, i.e. the loads applied to the right-hand side are being transmitted completely across the fracture. As can be seen from Table II, tibiae 6 and 7 (compression) show the highest FDR ratio, whereas tibia 3 (only four screws) shows the lowest.

## 4. Discussion

Starting from a stress-free situation, application of torque to the bone–plate structure does work on the structure; this is manifested as elastic strain energy within the system, the loads being so low that plastic deformation within the system would not occurr. This strain energy produces strains in the bone–screw–plate system which result in both bending and torsion.

The angulation of the fringes following the application of a point load midway between two supports indicated that the structure was not bending by simple out-of-plane deformation, but that some twisting was also occurring. If the system was responding in pure bending, then only out-of-plane displacement would occur, resulting in all of the fringes being vertical, as shown in Fig. 1. If pure torque was applied to a cylinder the interference fringes would diverge from left to right, also shown in Fig. 1. The holograms presented in Section 3 indicate that two types of displacement (bending and torsion) commonly occurred simultaneously in the systems studied, as a result of their complicated geometry.

By applying a load to the bone–screw–plate structure and recording a double-exposure hologram, the interference fringes provide information about the deformation of the object without contacting the object and with a high accuracy. The technique is sufficiently sensitive to record changes in the fracture configuration: whether the bone ends were in contact, compression or distracted. Using any other techniques it would be extremely difficult to detect strain produced by bending and by torsion over the whole bone surface. The torque loading method was found to be more repeatable than applying three-point bending; however, it was recognized that the end conditions were still critical in the final results. It was recognized that the fringe density for a given load was far too sensitive to the end conditions and the loading conditions to be able to record meaningful fringe densities. The results could only be analysed by comparing fringe densities, or fringe separations, relative to other

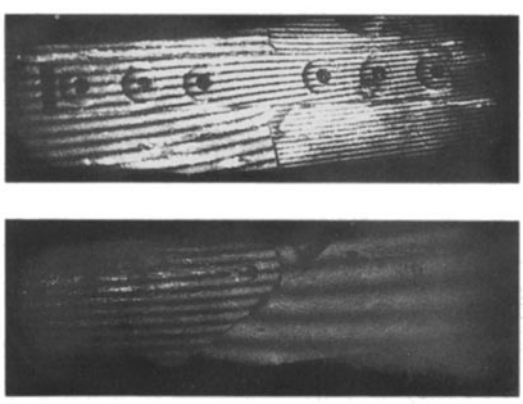

*Figure 7* Reconstructed image from hologram of tibia 5. Torsional loading is transmitted across the natural fracture with little out-of-plane bending, and reduced relative movement at the fracture site.

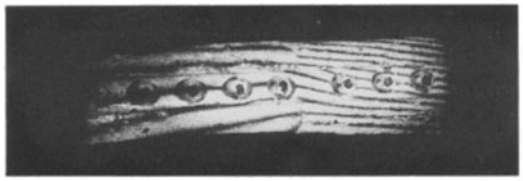

*Figure 9* Reconstructed image from hologram of tibia 7. Compression was applied across the fracture site using an AO narrow dynamic compression plate, shown to be less effective by the lower fringe density ratio (FDR) across fracture site.

fringe densities within the same hologram. The absolute displacements of the bone–screw–plate systems were not analysed quantitatively, due to the difficulties mentioned, but the relative displacements between different parts of the system were investigated and, as the technique was non-destructive, the testing could be continued after measurement. Direct comparisons between different bones (without the complication of different bone shapes and sizes, etc.) were not possible, but comparisons within each bone were possible.

The application of a bending moment to a fractured tibia–plate structure showed that there was a difference in the fringe density at the fracture site between the bone and the plate. This was also observed [14, 19] when whole tibiae were loaded in cantilever bending; the fringes were found to coincide away from the fracture site, but not in the centre. This finding indicated that there was relative movement between the plate and the bone between the inner screws, at the point in a broken bone where maximum stability is required for complete immobilization of the fracture site if rigid internal fracture fixation is to be attained. The importance of friction between the plate and the bone has been identified [22] as being important in fracture repair, as it allows the loads partially to bypass the plate, making it less likely to fail in clinical use. However, as shown in the holograms, it can be seen that over the central portion of the plate the friction effect was greatly reduced, and hence the loading of the plate would be higher and failure more likely.

Testing fracture fixation systems in torsion has been reported in only one paper before this work [19], in which it was found that a dried tibia with an eight-hole AO dynamic compression plate applied across a transverse osteotomy became less stiff if the two central screws were removed. The results presented here extended this observation by investigating the difference between transverse fracture, with a "natural" fracture surface, and to include the role of compression across the fracture site. Carrying out the analysis on the torsional stiffness of the system is not only more sensitive, but also relevant to the clinical application. It has been shown that the torsional stiffness of a fracture fixation system is important in maintaining the overall rigidity [3]. Assuming that an accurate reduction of the fracture has been carried out, and compression applied across it, then initially the least-stiff and most-critical loading direction will be torsional. It was concluded [23] that the bending stiffness of a fracture fixation system was important only in the application of compression across the fracture site, whereas the torsional stiffness was important in eliminating relative movement at the bone fragment ends. The discontinuity of fringes in the holograms across the fracture site indicated that a small amount of movement was occurring there even at very small loads. This result is important, as interfragmentary movement influences the healing pattern of cortical bone. The assumption is made in rigid fracture fixation that absolute immobilization of the fracture ends occurs and hence direct bone healing takes place. It is clear from these highly sensitive measurements using holographic interferometry that complete immobilization is not, in fact, occurring even when compression is applied across the fractured surfaces. This questions the amount of movement or strain that the bone cells are able to tolerate and still produce direct callus, rather than producing bone which leads to indirect fracture repair.

Torsional loads produce shear at the fracture surfaces, which can be counteracted only by friction or interdigitation of the surfaces [24]. The holograms presented in Fig. 7 show that some of the relative movement between fracture ends was eliminated by the interdigitation, but that shear was still occurring between the ends despite accurate reduction. The only reliable method of reducing the shear effect between the fracture ends was found to be compression, producing friction between the bone ends. Figs 8 and 9 showed the effects of applying compression, but also highlight the inherent problems of the technique. Applying effective compression across the fracture is clearly an extremely skilled art, and small variations in the way in which a plate is applied lead to a less satisfactory result, as shown in Fig. 9.

Introduction of the FDR illustrates the important aspects of the torsional rigidity of the various systems tested. The system that showed the highest FDR value, i.e. the closest to eliminating shear between the fracture ends, was the tibia with an eight-hole Osteo plate and compression applied. An angled osteotomy rather than a transverse one increased the torsional rigidity of the system. The angled fracture produced what might be considered to be one large interdigitation. As a torque was applied to the left hand side of the bone, twisting brought the bone into contact with the opposing end, thus preventing further movement and hence increasing the torsional rigidity of the system. In this instance the plate was the only restraint. However, when a natural fracture was fixed, the interdigitation of the fracture ends led to a higher FDR than for the angled osteotomy, indicating that the interaction of several angles was more effective in increasing the torsional stiffness. The tibia with a four-hole plate showed the least torsional stiffness, highlighting the need for compression between the plate and the bone and across the fracture site.

## 5. Conclusions

Holography has been shown to be a useful tool in the analysis of internal fracture fixation systems. The technique has illustrated features relevant to the systems, which have not been identified previously. The holographic interference patterns indicate the disturbance that occurs in the loading patterns of a structure when a plate links the two halves. Introducing compression at the fracture site has been shown to be important in increasing the torsional rigidity of the overall structure, and in maintaining stability of the fracture ends as cyclic loads were applied. If absolute immobilization of the fracture site is the aim of the fixation technique, then the importance of the surgeon's ability to reduce a fracture accurately was highlighted during this series of tests. It may be concluded that in order to establish load transfer across the

fracture site and for the structure to maintain the relative immobilization of the fracture ends following cyclic loading, the fracture ends should intedigitate closely and a large compressive load should also be applied across the fracture ends. If this is not achieved there will be movement between the fracture ends, the plates will consequently experience larger loads and the strains on the repair material will be much higher.

## Appendix A

The feasibility of holography was first set down and proved by Gabor in 1948. It allows the reproduction of a wavefront of light scattered by a three-dimensional object, by recording the intensity and phase of the light that is reflected from the object. A record of this object wave, compared to a reference beam, is made on a photographic emulsion, which subsequently allows a reconstruction of the object in three dimensions.

A beam from a laser, producing both monochromatic and temporally coherent light, is split into two parts known as a reference beam and an object beam, as shown in Fig. 1. The reference beam is directed via a series of mirrors and through a diffuser, on to the photographic plate. The object beam is directed along a pathway of identical length, through a diffuser, and on to the object; this beam is scattered and some of the reflected light falls on the photographic plate. The photographic plate is exposed to the reference and object beams simultaneously, and the interference between the beams appears as a diffraction pattern which constitutes a hologram.

The hologram can be viewed by replacing the processed photographic plate in the same position as had been used to record it, and illuminating it using the reference beam only. The virtual* image of the object can be seen by looking through the plate, which shows an image in three dimensions identical to the original object. It is possible to record the hologram by photographing either the virtual or the real† image, but photography loses the information on the phase of the light.

If one views the superposition of light from the reference and object beams, through a hologram, then the interference between two wavefronts occurs, provided that the processed holographic plate has been replaced exactly in its original position (to the nearest quarter-wavelength of light) and that the photographic emulsion has suffered minimal shrinkage during the developing sequence. Then when the object is displaced slightly, a fringe pattern appears which is a result of the change in the phase of the real object wavefront relative to that recorded on the plate. This type of hologram is termed a "real-time" or "live" holographic interference pattern [21]. The fringe pattern depends on the type of deformation and the direction of viewing.

An alternative technique, which eliminates the problem of precise repositioning, is known as the "frozen fringe" or "double-exposure" hologram. The plate is never disturbed during the recording phase of this method, and practically it is easier to use than the real-time method. The initial stages of recording this type of hologram are similar to that for a live hologram. A hologram of an object is recorded in its undeformed state. The object is then deformed or undergoes a small displacement, and a second exposure is taken on the same plate. When processed the hologram reconstructs both images, which interfere with each other and appear as dark stripes superimposed on the image of the object, known as interference fringes. A single double-exposure hologram records one loading condition and can be viewed in the absence of the object.

## Appendix B: The zero-fringe method

The following equation describes the general case for relating the fringe order to the displacement.

$$n\lambda = \Delta \tag{B1}$$

where $\Delta$ is the change in the optical path length, $n$ is the fringe order and $\lambda$ is the wavelength of light. If the viewing and illumination direction are the same and the displacement is in the direction of viewing also, then

$$n\lambda/2 = u_z \tag{B2}$$

where $u_z$ is the out-of-plane displacement. Provided the object surface is perpendicular to the viewing direction, then the out-of-plane displacements can be found directly from the fringe order.

If the line of sight is not in the direction of movement of the object, the magnitude of the actual displacement is given by

$$u = \frac{n\lambda}{2\cos\Omega} \tag{B3}$$

where $\Omega$ is the angle between the line of sight and the direction of the displacement.

If the illumination and viewing directions are not coincident but are at angle $\phi$, then the zero-fringe technique gives the component along the bisector of that angle by

$$u_{\phi/2} = \frac{n\lambda}{2\cos(\phi/2)\cos\Omega} \tag{B4}$$

The order of the fringe can be determined only if the zero-order fringe is in the field of view. However, although absolute displacements require a knowledge of the geometry of the system that has produced the hologram, if absolute displacements are not required and it is assumed that only out-of-plane displacements are occurring, the situation is simplified even further, since the zero-order fringe is no longer required. This is the situation that occurs when relating the displacement of bones considered in this work.

Assuming that the illumination and viewing directions are the same, then the difference between the displacements of two points P and Q in the direction of the line of sight, can be found from the absolute

*Virtual image: one generated in front of the plate due to divergence of beams.
†Real image: one generated behind the holographic plate.

displacements of P and Q; namely $u_p$ and $u_q$ are given by

$$u_p = n_p\lambda/2 \quad \text{and} \quad u_q = n_q\lambda/2 \qquad \text{(B5)}$$

where $n_p$ and $n_q$ are the fringe orders at P and Q.

By subtracting the equations in Equation B5, the difference between the two points gives

$$u_z = \frac{(n_p - n_q)\lambda}{2} \qquad \text{(B6)}$$

i.e. the displacement of the point P relative to the point Q is the number of fringes between P and Q multiplied by $\lambda/2$.


## Acknowledgements

The funding for one of the authors (J.S.) by the SERC and Johnson & Johnson Orthopaedics Ltd, during this work is gratefully acknowledged. Many thanks to Dr G. P. Evans and Dr D. L. Bader for their helpful comments in the preparation of this paper.


## References


1. G. W. BRADLEY, G. M. McKENNA, H. K. DUNN, A. U. DANIELS and W. O. STATTON, *J. Bone Joint Surg.* **61A** (1979) 866.
2. R. E. COUTTS, W. H. AKESON, S. L.-Y. WOO, J. V. MATTHEWS, M. GONSLAVES and D. AMIEL, *Orthop. Clin. N. Amer.* **7** (1976) 223.
3. S. L.-Y. WOO, B. SIMON, W. AKESON, M. GOMEZ and Y. SEGUCHI, *J. Biomed. Res.* **17** (1983) 427.
4. A. U. DANIELS, L. CONE and R. SCHULTZ, in Proceedings 31st Annual ORS, Las Vegas, Nevada, 21 to 24 January 1985, p. 164.
5. W. H. AKESON, R. D. COUTTS and S. L.-Y. WOO, *Can. J. Surg.* **23** (1980) 235.
6. D. G. BAGGOTT, A. E. GOODSHIP and L. E. LANYON, *J. Biomech.* **10** (1981) 701.
7. R. PILLIAR, H. CAMERON, A. BINNINGTON, J. SZIVEK and I. MACNAAB, *J. Biomed. Mater. Res.* **13** (1979) 799.
8. E. CHEAL, W. HAYES, A. WHITE and S. PERREN, *Comput. Struct.* **17** (1983) 141.
9. R. PLANT and D. BARTEL, *Adv. Bioeng.* (1974) 85.
10. B. R. SIMON, S. L.-Y. WOOD, G. M. STANLEY, S. R. OLMSTEAD, M. McCARTY and G. JEMMOTT, *J. Biomech.* **10** (1977) 79.
11. K. TAYTON, C. JOHNSON-NURSE, B. McKIBBIN, J. BRADLEY and G. HASTINGS, *J. Bone Joint Surg.* **64A** (1982) 105.
12. K. PIWERNETZ. in "Holography in Medicine and Biology", edited by G. Von Bally (Springer-Verlag, Berlin, 1971) p. 7.
13. M. T. MANLEY, J. GURTOWSKI, L. STERN, M. HALIONA and T. BOWLINS, in Proceedings of 29th Annual ORS, California, 8 March 1983.
14. U. HANSER, in "Holography in Medicine and Biology", edited by G. Von Bally (Springer-Verlag, Berlin, 1979) p. 27.
15. M. J. LALOR, D. GROVES and J. T. ATKINSON, *ibid.* p. 20.
16. D. VUKICEVIC, V. NIKOLIC, S. VUKICEVIC, J. HANCEVIC and Z. SUCUR, *ibid.* p. 34.
17. T. MATSUMOTO and F. FUJITA, in Proceedings of International Conference, Graz, Austria: "Optics in Biomedical Sciences", edited by G. Von Bally and P. Greguss (Springer-Verlag, Berlin, 1982).
18. T. MATSUMOTO, A. KOJIMA, R. OGAWA, K. IWATA and R. NAGATA, in Proceedings of International Conference on Holographic Applications, China, Beijing, 1986.
19. V. HANSER, J. HARMS and H. MITTELMEIER, *Med.-orthop. Technik* **2** (1974) 47.
20. A. KOJIMA, R. OGAWA, N. IZUCHI, T. MATSUMOTO, K. IWATA and R. NAGATA, in Proceedings of 5th Meeting of European Society of Biomechanics, edited by G. Bergman, R. Kobel and A. Rohlman (Martinus Nijhoff, Dordrecht, 1987).
21. C. M. VEST, "Holographic Interferometry" (Wiley, New York, 1979).
22. J. SCHATZKER, *Can. J. Surg.* **23** (1980) 232.
23. S. G. STEINEMAN, in "Biomaterials and Biomechanics", edited by P. Ducheyne, G. Van der Perre and A. E. Aubert (Elsevier Science, 1983).
24. S. M. PERREN and B. A. RAHN, *Orthop. Survey* **2** (1978) 108.



*Received 5 December 1989*
*and accepted 19 April 1990*